ISSN 2706-6819 Vol.8, Issue 2: 11-24, DOI: 10.25236/IJFM.2026.080202

Dendrobium nobile Lindley Ameliorates Psoriasis-Like Dermatitis by Modulating Keratinocyte Differentiation and Myeloid Leukocyte Activation

Huan Li[1,2,a], Ziyue Zhou[2,3,b], Qiuyang Chen[2,3,c], Lei Shi[2,3], Jingyuan Ma[2,3], Xingyue Li[2,3], Zhiyang Yu[2,3], Ying Yang[4], Jie Jing[1,d,*]

[1]School and Hospital of Stomatology, Zunyi Medical University, Zunyi, Guizhou, China
[2]The Collaborative Innovation Center of Tissue Damage Repair and Regeneration Medicine of Zunyi Medical University, Zunyi, Guizhou, China
[3]Department of Burns and Plastic Surgery, Affiliated Hospital of Zunyi Medical University, Zunyi, Guizhou, China
[4]Department of Dermatology, The Second Affiliated Hospital of Zunyi Medical University, Zunyi, Guizhou, China
[a]1315207329@qq.com, [b]1024454417@qq.com, [c]1079216569@qq.com, [d]JieJing@zmu.edu.cn
**Corresponding author*

Abstract: *This study explored the therapeutic effects and underlying mechanisms of polysaccharides and alkaloids from Dendrobium nobile Lindley (DNL) on psoriasis. An imiquimod (IMQ)-induced psoriasis mouse model was established to observe the pharmacological effects of DNLPs and DNLAs. The assessments included Psoriasis Area and Severity Index scoring, hematoxylin-eosin (HE) staining and immunohistochemistry, tyramide signal amplification, reverse transcription-quantitative polymerase chain reaction, and RNA sequencing (RNA-seq). The results showed that oral administration of DNLPs and DNLAs could effectively alleviate psoriasis symptoms and improve histopathological features. Transcriptomic analysis indicated that both components regulated immune responses and cellular functions, thereby reducing local inflammation through inhibition of myeloid leukocyte infiltration. Immunofluorescence results also verified that the expression of keratin markers K14, K16 and K17 was significantly downregulated, along with decreased levels of macrophage and neutrophil markers in the treatment groups. In conclusion, DNLPs and DNLAs exert prominent anti-inflammatory effects via modulating keratinocyte differentiation and suppressing the excessive activation of myeloid leukocytes. These findings provide a solid theoretical basis for the clinical application of Dendrobium nobile Lindley components in psoriasis therapy.*

Keywords: *Psoriasis, Dendrobium nobile Lindley, Plant extract, RNA sequencing analysis, Keratinocyte, Myeloid leukocyte*

1. Introduction

Psoriasis is a chronic inflammatory disease with a prevalence of approximately 2–3%, affecting over 125 million people worldwide [1-3]. Psoriasis presents as well-defined erythematous plaques with silver-white scaling. Its main histopathological feature is acanthotic thickening, often seen at sites of epidermal trauma (e.g., elbows, knees, back, and trunk); however, it can affect any skin area, significantly reducing patients' quality of life [4, 5]. Current therapeutic approaches for psoriasis include topical treatments, systemic medications, immune modulation, and biologic agents, such as tumour necrosis factor-alpha (TNF-α) inhibitors, interleukin (IL)-12/IL-23 inhibitors, and IL-17 inhibitors. These therapies are characterised by marked efficacy and favourable safety profiles, offering additional therapeutic options for patients with suboptimal responses to traditional treatments [5, 6].

Traditional Chinese herbs (TCHs) effectively minimise the associated side effects, and many TCH therapies have been widely applied in clinical practice [7]. The most commonly used TCHs for the treatment of psoriasis include *Salvia miltiorrhiza* Bunge, *Spatholobus suberectus* Dunn, *Paeonia lactiflor*a Pall., *Isatis tinctoria* L., *Scutellaria baicalensis* Georgi, *Paeonia* × *suffruticosa* Andrews, *Arnebia euchroma* (Royle) I.M.Johnst., *Tripterygium wilfordii* Hook. f., *Lithospermum erythrorhizon* Siebold & Zucc. [8-10]. In recent years, the application of TCH in psoriasis treatment and the mechanisms

ISSN 2706-6819 Vol.8, Issue 2: 11-24, DOI: 10.25236/IJFM.2026.080202

of action have been extensively studied. The therapeutic effects of several TCHs in psoriasis have been experimentally validated. Representative herbs include *Angelica dahurica* (Hoffm.) Benth. & Hook.f. ex Franch. & Sav., *Rhododendron indicum* (L.) Sweet, *Premna herbacea* Roxb., *Rosmarinus officinalis* L., and Jingfang granules [11-15].

Dendrobium nobile Lindley (DNL), a traditional Chinese medicinal herb, contains various chemical components, including polysaccharides, phenanthrenes, sesquiterpenoids, and alkaloids, the pharmacological activities of which are closely related to these substances. It exhibits a broad spectrum of pharmacological effects, such as anti-tumour, anti-ageing, immune-enhancing, hypoglycaemic, and anti-cataract effects [16, 17]. Polysaccharides and alkaloids are the primary bioactive substances responsible for these effects, particularly their anti-tumour, anti-hypertensive, neuroprotective, immunoregulatory, antioxidative, and anti-inflammatory activities [18, 19]. Although current therapies effectively control the inflammatory processes in psoriasis, prolonged immunosuppressive therapy can increase susceptibility to infections and skin malignancies [4, 5, 20].

To date, no studies have investigated the role of DNL in the pathogenesis of psoriasis. Therefore, applying modern research approaches and technologies to investigate the biological activities of DNL may not only enhance our understanding of its pharmacological mechanisms but also provide novel therapeutic strategies for psoriasis management. In this study, we extracted the primary functional components, polysaccharides (DNLPs) and alkaloids (DNLAs), from DNL to investigate their effects on psoriasis and elucidate their potential mechanisms of action, providing a scientific foundation for their topical application in psoriasis treatment.

2. Material and methods

2.1 Imiquimod (IMQ)-induced psoriasis-like mouse model

SPF male C57BL/6J mice (6–8 weeks old, weighing 22–25 g) were purchased from Scilab Biotechnology Co., Ltd. (Henan, China) (license number SCXK(Yu)2020-0005). This study was approved by the Zunyi Medical University Laboratory Animal Welfare Ethics Committee (approval number: ZMU21-2404-801, 25 April 2024). Based on a literature review, we used a DNLP concentration of 100 mg/kg [21, 22] and a DNLA concentration of 80 mg/kg [23, 24]. A total of 21 mice were randomly assigned to three groups based on their body weight: model control group, DNLP group (100 mg/kg; Xiya, Guangzhou biological), and DNLA group (80 mg/kg; Xiya, Guangzhou biological), with seven mice per group. The IMQ-induced psoriasis model is widely recognised as a standard method for studying psoriasis [25, 26]. The modelling procedure in this experiment was based on protocols established in previous research, outlined as follows: hair on the dorsal area of each mouse was shaved using an electric hair trimmer, and excess hair was removed using a depilatory cream, leaving an exposed skin area of approximately 2 × 3 cm. On the day of shaving, the shaved area was observed for signs of redness, swelling, or ulceration. Treatment with DNLPs and DNLAs commenced on day 0; the control group was administered double-distilled water. Psoriasis models were then induced by applying 50 mg (5%) IMQ cream (Sichuan Mingxin Pharmaceutical Co., Ltd., H20030129) to the exposed dorsal skin of the mice daily for six consecutive days after two days of pretreatment with DNLPs and DNLAs. The severity of skin lesions was assessed daily using the Psoriasis Area and Severity Index (PASI). Twenty-four hours after the final dose, the dorsal skin tissue from the lesioned area was collected for haematoxylin and eosin (H&E) staining, immunohistochemistry (IHC), immunofluorescence, reverse transcription-quantitative polymerase chain reaction (RT-qPCR) analysis, and RNA sequencing (RNA-seq).

2.2 H&E staining

Tissue samples were fixed in 4% paraformaldehyde for 48 h, embedded in paraffin, and stained with H&E. To quantify the thickness of the epidermis, dermis, and adipose layer, wax blocks were cut into 4-μm-thick sections using a microtome (Leica), mounted on ordinary slides (Citoglas), placed in an oven at 65 °C for 1 h, dewaxed, and rinsed with running water for 5 min. Staining was performed using a water-soluble H&E staining solution (Mayer). The specific procedure was as follows: haematoxylin staining was performed for 5–7 min, followed by differentiation in hydrochloric acid and alcohol for 2 s. Subsequently, the samples were placed in eosin solution for 3 min. The samples were then dehydrated using a gradient of ethanol, made transparent with xylene, and dried. The slides were sealed, and the thicknesses of the epidermis, dermis, and adipose layer were observed under a full-slide scanning microscope (VS200, Olympus). Measurements were performed using NIH/ImageJ software

ISSN 2706-6819 Vol.8, Issue 2: 11-24, DOI: 10.25236/IJFM.2026.080202

(https://imagej.net/NIH_Image).

2.3 IHC staining

Mouse skin tissue sections (prepared as described for H&E staining) were deparaffinised in xylene and rehydrated. Antigen retrieval was performed using Tris-EDTA (pH 9.0) at 95–100 °C for 12–18 min. After cooling to room temperature, endogenous peroxidase activity was blocked by incubating the sections with 3% hydrogen peroxide at room temperature for 15 min, followed by washing with phosphate-buffered saline (PBS). Nonspecific staining was blocked by incubation with a blocking solution at 37 °C for 30 min. The sections were then incubated overnight at 4 °C with the primary antibody Ki67 (1:400, D3B5, Cell Signaling Technology). Following incubation, the sections were equilibrated to room temperature for 45 min, washed with PBS, and incubated with the secondary antibody at 37 °C for 30 min. Following PBS washes, diaminobenzidine (DA1010, Solarbio) was used for colour development, which was terminated by washing with distilled water. The sections were then stained with haematoxylin (Beijing Coolaber, catalogue number SL7070-500mL) for 2–5 min and washed with water. Differentiation was performed using hydrochloric acid-ethanol (Shanghai Beyotime, catalogue number C0163M), followed by washing with water. The sections were subsequently dehydrated, cleared with xylene, and mounted with neutral gum for microscopic examination. For each mouse skin section, a random field was selected at 200× magnification. The cell nuclei were stained blue, and positive staining appeared brown. The positive cell rate in each field was quantified using ImageJ software and statistically analysed.

2.4 Tyramide signal amplification

Formalin-fixed and paraffin-embedded mouse skin samples were cut into 4-μm-thick sections and mounted on adherent slides. The slides were deparaffinised according to a standard protocol and sequentially rehydrated in xylene, ethanol, and pure water. The samples were boiled in 10 mM citrate buffer (pH 6.0) or ethylenediaminetetraacetic acid (pH 9.0) for 16 min for antigen repair. After cooling to room temperature, the slides were incubated with 3% hydrogen peroxide endogenous peroxidase blocker for 15 min at room temperature, protected from light, and subsequently rinsed with PBS; the slides were then sealed at 37 °C for 30 min using 10% goat serum (Service Bio), followed by dropwise addition of the primary antibody, and placed in an incubator at 4 °C for overnight incubation. Primary antibody concentrations were used as follows: keratin (K)14 (1:1000, Sc-53253, Santa Cruz Biotechnology); K16 (1:600, PAB35308, Bioswamp); K17 (1:800, BS48564-25, Bioworld); CD206 (1:4000, 18704-1-AP, Proteintech); iNOS (1:200, A3774, Abclonal); and Ly-6g (1:600, PAB52649, Bioswamp). Sections were maintained at room temperature for 45 min, rinsed in PBS, and then titrated with secondary antibody, incubated for 30 min at 37 °C, and rinsed again in PBS. A fluorescent dye was applied and incubated for 15 min at room temperature, protected from light, and then rinsed in PBS. Cell nuclei were stained with DAPI (Solarbio), and coverslips were mounted onto slides using an antifading mounting medium (S2110; Solarbio). Negative controls were prepared in the same manner, with PBS replacing the primary antibody. The completed sections were observed under a fluorescence microscope and analysed using ImageJ software.

2.5 RT-qPCR

Fresh dermal specimens (10–20 mg) were rinsed three times with PBS, followed by precise dissection using sterilised microsurgical scissors. Nucleic acid isolation was performed using the Novizyme RNA isolation kit protocol, with strict adherence to the manufacturer's specifications. The purified RNA lysate was aliquoted into sterile microcentrifuge tubes for quantitative assessment using a NanoDrop spectrophotometer.

For cDNA synthesis, precisely 500 μg of quantified RNA was aliquoted into PCR-compatible tubes. Following genomic DNA supplementation, thermal cycling was conducted under specified conditions: primary incubation at 42 °C (120 s), followed by the reverse transcription protocol at 50 °C (15 min), concluding with enzyme inactivation at 85 °C (5 s). The synthesised cDNA products were cryopreserved at -80 °C for long-term storage before downstream applications.

Quantitative PCR (qPCR) was performed using 10-fold diluted cDNA templates. The thermal profile comprised three distinct phases: initial denaturation at 95 °C (30 s), 40 amplification cycles with dual-temperature cycling (95 °C/10 s → 60 °C/30 s), and final melt curve analysis (95 °C/15 s → 60 °C/60 s → 95 °C/5 s). Post-amplification data acquisition and subsequent 2-ΔΔΔCT computational analysis

ISSN 2706-6819 Vol.8, Issue 2: 11-24, DOI: 10.25236/IJFM.2026.080202

enabled the comparative quantification of target gene expression levels. The primers used for RT-qPCR are listed in Table 1.

Table 1: Sequences of primers for RT-qPCR

Primer		Sequences
Mouse IL-1β	Forward	5'- AGTTGACGGACCCCAAA -3'
	Reverse	5'- TCTTGTTGATGTGCTGCTG -3'
Mouse IL-17α	Forward	5'- TCGAGAAGATGCTGGTGGGT -3'
	Reverse	5'- CTCTGTTTAGGCTGCCTGGC -3'

2.6 RNA-seq

Total RNA was isolated using TRIzol reagent (Invitrogen). RNA degradation and contamination were assessed using 1% agarose gel electrophoresis. RNA purity was evaluated using a NanoPhotometer spectrophotometer (IMPLEN, CA, USA). RNA integrity was determined using an RNA Nano 6000 Assay Kit on a Bioanalyzer 2100 system (Agilent Technologies, CA, USA). For RNA sample preparation, 1 μg of RNA per sample was used as the input material. Sequencing libraries were prepared using the NEBNext® Ultra™ RNA Library Preparation Kit for Illumina® (NEB, USA), following the manufacturer's instructions. This kit uses fragmented mRNA as a template and random oligonucleotides as primers to synthesise the first strand of cDNA in an M-MuLV reverse transcriptase system. The RNA strand was then degraded using RNase H, and the second strand of cDNA was synthesised from dNTPs using a DNA polymerase I system. After purification, the double-stranded cDNA was subjected to end repair, A-tailing, and ligation using sequencing adapters. Approximately 250–300 bp of cDNA was selected using AMPure XP beads and amplified by PCR; the PCR products were purified again using AMPure XP beads, ultimately yielding the library. The Illumina NovaSeq PE150 sequencing strategy was used for libraries that passed quality control.

After quality control, the DESeq2 R package was used for differential gene expression analyses. Kyoto Encyclopedia of Genes and Genomes (KEGG) pathway and Gene Ontology (GO) term enrichment analyses of differentially expressed genes (DEGs) were performed using ClusterProfiler R software, and the statistical significance threshold was set at $P < 0.05$.

2.7 Statistical methods

Except for the analysis software used for annotation, data processing and statistical analyses were performed using GraphPad Prism 8.0 software (GraphPad Software, USA). Numerical data are expressed as the mean ± standard deviation. For comparisons between multiple groups, one-way analysis of variance was used, followed by Tukey's post hoc multiple comparison test. Statistical significance was set at $P < 0.05$.

3. Results

3.1 DNLP/DNLA treatment alleviated skin lesions in IMQ-induced psoriasis-like dermatitis in mice

To confirm the therapeutic effects of DNLPs/DNLAs (100 and 80 mg/kg, respectively) on psoriatic lesions, mice were intragastrically administered DNLPs/DNLAs. Two days later, IMQ cream was applied to establish a psoriasis-like mouse model (6 days, 50 mg) (Figure 1A, 1B). DNLPs and DNLAs reduced the skin thickness and PASI scores of back lesions (Figure 1C, 1D). Additionally, the mRNA levels of the pro-inflammatory cytokines IL-17α and IL-1β were downregulated in the DNLP and DNLA treatment groups (Figure 1E). Histopathological analysis revealed that DNLPs/DNLAs alleviated IMQ-induced epidermal hyperplasia, acanthosis, and hyperkeratosis. H&E staining revealed that the spinous thickness was significantly thinner in the experimental group than in the control group (Figure 1F, 1G). Hyperkeratosis and parakeratosis are important pathological features of psoriasis, and Ki67 is a nuclear antigen that serves as a marker for cell proliferation [27, 28]. IHC showed that in lesional skin, the increased numbers of Ki67 cells that developed in the IMQ group were markedly diminished in the DNLP- and DNLA-treated groups (Figure 1F, 1G). In conclusion, DNLPs and DNLAs demonstrated significant therapeutic effects against IMQ-induced psoriasis-like dermatitis in mice by attenuating abnormal keratinocyte proliferation and excessive inflammation.

ISSN 2706-6819 Vol.8, Issue 2: 11-24, DOI: 10.25236/IJFM.2026.080202

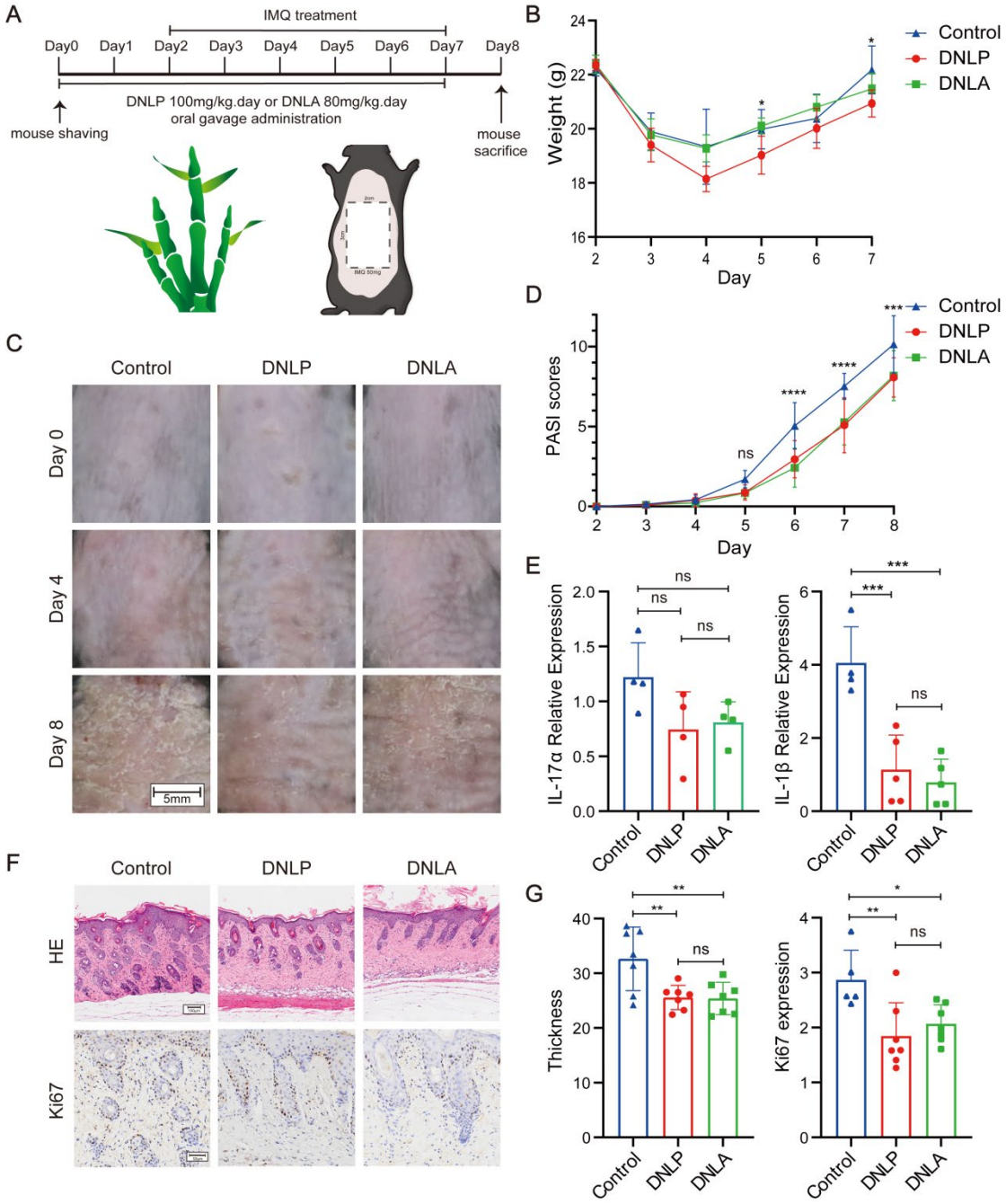

*Figure 1: DNLP/DNLA treatment ameliorates IMQ-induced psoriatic skin lesions. (A) Mice were pretreated with DNLPs or DNLAs by oral gavage for 2 days, followed by topical IMQ application to the dorsal skin for 6 consecutive days. Dosages and treatment areas are as indicated in the figure. (B) Body weight was measured and recorded daily using an electronic balance. (C) Dorsal skin was imaged on days 0, 4, and 8 to document psoriasiform changes; scale bar = 5 mm. Mice in the treatment groups showed milder phenotypic symptoms. (D) Disease severity was assessed daily using the PASI, with composite scores for erythema, scaling, and dermal infiltration. Data are presented as mean ± SD (n = 7 per group). (E) The effects of DNLPs and DNLAs on the mRNA expression of the inflammatory genes Il-17a and Il-1β were determined by RT-qPCR. (F) DNLP/DNLA treatment ameliorates IMQ-induced histopathological abnormalities in psoriatic skin lesions. (F, G) H&E staining reveals that DNLP and DNLA treatment reduces epidermal hyperplasia. Original magnification ×200, scale bar = 100 μm. Representative images and quantification of Ki67-positive cells by immunohistochemistry are presented. Original magnification ×400, scale bar = 50 μm. Data are presented as mean ± SD. *P < 0.05, **P < 0.01, ***P < 0.001 vs. the IMQ-treated model group; ns, not significant.*

ISSN 2706-6819 Vol.8, Issue 2: 11-24, DOI: 10.25236/IJFM.2026.080202

3.2 Characterisation of DNLP-treated skin lesions via RNA-seq analyses

To reveal the potential mechanism by which DNLPs and DNLAs alleviate skin inflammation, six transcriptomes of two skin lesion samples from the IMQ and DNLP groups were generated using the Illumina high-throughput sequencing platform. In the control group, the average number of raw reads obtained was 4.56×10^7, and the average number of clean reads obtained after filtering was 4.52×10^7, with an average Q20 of clean reads above 98.64%. In the DNLP group, the average number of raw reads obtained was 5.26×10^7, and the average number of clean reads obtained after filtering was 5.21×10^7, with an average Q20 of clean reads above 98.6%. Principal component analysis revealed a clear distinction between the groups, demonstrating that model establishment and drug intervention influenced the transcriptional profiles (data not shown). There were 2738 DEGs in the DNLP group compared with those in the control group (1416 upregulated and 1322 downregulated). The 14 DEGs most notably upregulated and downregulated following DNLP treatment are shown in Figure 2A. Figure 2B shows a heatmap following additional cluster analysis of psoriasis-related genes, demonstrating that DNLPs significantly downregulated the expression of interleukins, such as IL-1β, IL-17α, and K5, K14, K16, and K17. GO function enrichment analysis (Figure 2C) showed that, compared with those in the model group, the DEGs in the DNLP group were mainly enriched for leukocyte migration and myeloid leukocyte activation. KEGG analysis indicated that the DEGs between the DNLP and control groups mainly included lysosomes, ribosomes, and T helper 17 cell (Th17) differentiation (Figure 2D).

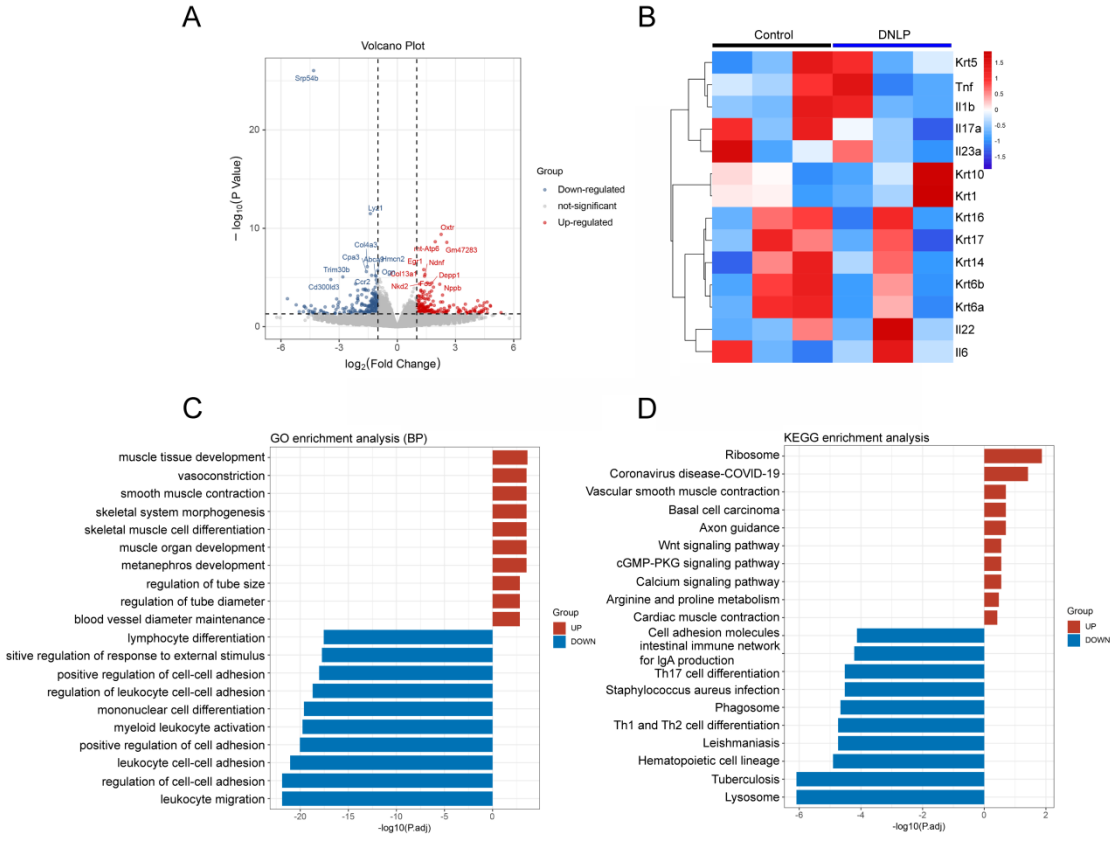

Figure 2: Differentially expressed genes (DEGs) in psoriatic lesions of mice following treatment with 100 mg/kg DNLP. (A) Volcano plot illustrating the distribution of differentially expressed mRNAs. Blue dots represent downregulated mRNAs, red dots represent upregulated mRNAs, and grey dots represent mRNAs with no significant differential expression. (B) Heatmap showing all differentially expressed mRNAs in psoriatic lesions from DNLP-treated mice (n = 3) compared with control mice (n = 3), for which all adjusted P-values < 0.05 and |Log2FC| > 1. Red indicates upregulated genes, and blue indicates downregulated genes. (C) Top 20 enriched Gene Ontology (GO) pathways of DEGs. (D) Top 20 enriched Kyoto Encyclopedia of Genes and Genomes (KEGG) pathways of DEGs.

3.3 Characterisation of DNLA-treated skin lesions via RNA-seq analyses

We identified the DNLA targets in the same manner as those of DNLP. There were 5.29×10^7 raw reads, 5.25×10^7 clean reads, and an average Q20 of clean reads > 98.67% in the DNLA group. There

ISSN 2706-6819 Vol.8, Issue 2: 11-24, DOI: 10.25236/IJFM.2026.080202

were 3021 DEGs in the DNLA group compared with those in the IMQ group (1527 upregulated and 1494 downregulated). The 14 DEGs that were most notably upregulated and downregulated are shown in Figure 3A. Figure 3B shows a heatmap following additional cluster analysis of psoriasis-related genes, demonstrating that DNLAs significantly downregulated the expression of interleukins, K14, K16, K17, and S100 protein-related genes. GO functional enrichment analysis (Figure 3C) showed that the DEGs in the DNLA group were mainly enriched for extracellular matrix organisation and myeloid leukocyte activation. KEGG analysis showed that the DEGs between the DNLA and IMQ groups mainly included the chemokine signalling pathway and Th1, Th2, and Th17 cell differentiation (Figure 3D).

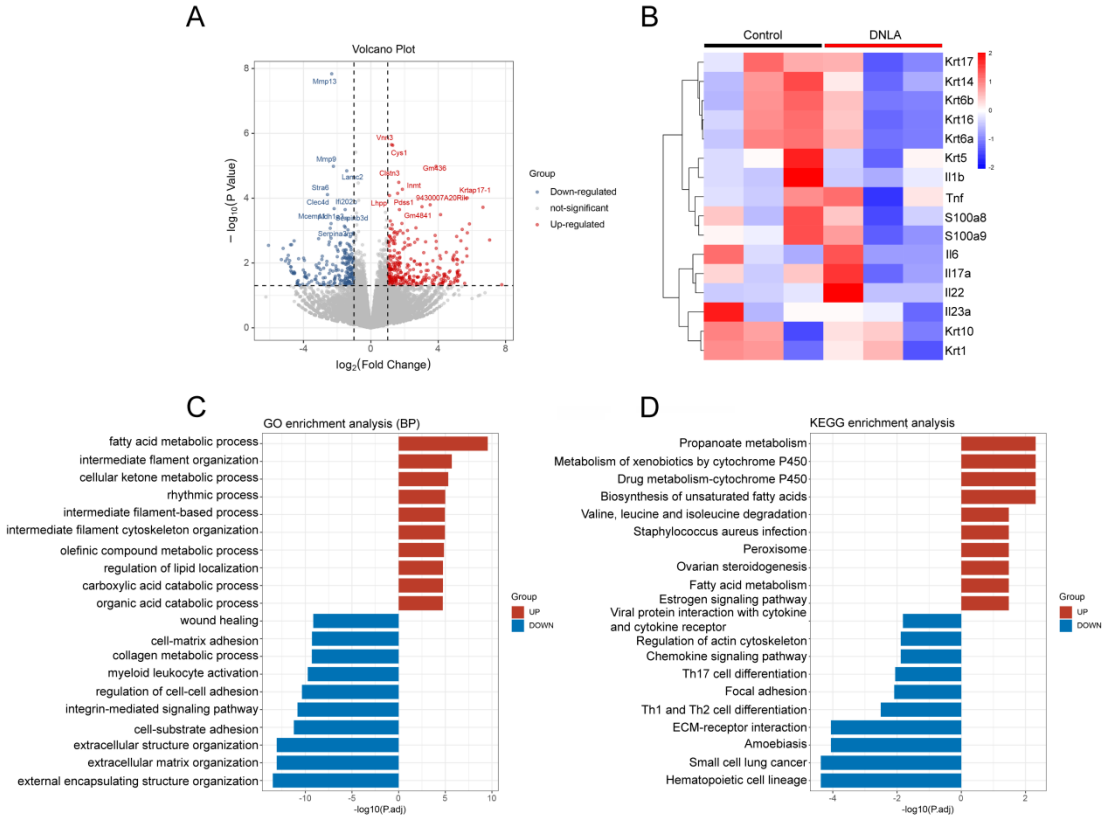

Figure 3: Differentially expressed genes (DEGs) in psoriatic lesions of mice following treatment with 80 mg/kg DNLAs. (A) Volcano plot illustrating the distribution of differentially expressed mRNAs. Blue dots represent downregulated mRNAs, red dots represent upregulated mRNAs, and grey dots represent mRNAs with no significant differential expression. (B) Heatmap showing all differentially expressed mRNAs in skin lesions from DNLA-treated mice (n = 3) compared with control mice (n = 3), for which all adjusted P-values < 0.05 and |Log2FC| > 1. Red indicates upregulated genes, and blue indicates downregulated genes. (C) Top 20 enriched Gene Ontology (GO) pathways of DEGs. (D) Top 20 enriched Kyoto Encyclopedia of Genes and Genomes (KEGG) pathways of DEGs.

3.4 Characterisation of DNLP and DNLA effects on psoriatic skin lesions via RNA-seq analyses

To further identify the molecular mechanisms by which DNLPs and DNLAs alleviate skin inflammation, we used DESeq2 with a filter criterion of log fold change >1 and $P < 0.05$ to identify DEGs. Compared with those in the control group, 1254 and 332 specific DEGs were identified in the DNLP and DNLA groups, respectively, with 93 overlapping DEGs between the two groups (Figure 4A). Figure 4B shows a heat map of the DEGs after clustering analysis, illustrating the expression patterns of DEGs in the control, DNLA, and DNLP groups. Red represents high expression, and blue represents low expression. The significant changes in gene expression following DNLP and DNLA treatment further highlight the distinct effects of these treatments on modulating gene expression related to skin inflammation. As shown in Figure 4B, the DEGs were mainly associated with immune cell activation, including *Clec2e*, *H2-Aa*, *CD83*, and *CD86* [29-31]. Additionally, *HAS1* and *Mmp13* are related to skin and tissue damage repair, and *Fos* and *DUSP1* are involved in inflammatory responses [32-35].

Figure 4C presents the results of GO and KEGG enrichment analyses for the DEGs shared between DNLPs and DNLAs. GO enrichment analysis (top panel) revealed that these DEGs were significantly

ISSN 2706-6819 Vol.8, Issue 2: 11-24, DOI: 10.25236/IJFM.2026.080202

enriched in immune-related biological processes, including antigen processing and presentation, cell–cell adhesion, and T cell activation. KEGG pathway enrichment analysis (bottom panel) showed that these DEGs were primarily involved in various immune- and inflammation-related pathways, such as 'rheumatoid arthritis', 'Th17 cell differentiation', and 'autoimmune thyroid disease'.

Overall, these results indicate that DNLPs and DNLAs share a common mechanism for modulating immune responses and cellular processes in psoriasis. This suggests that they alleviate psoriasis-related inflammation by influencing myeloid leukocyte infiltration.

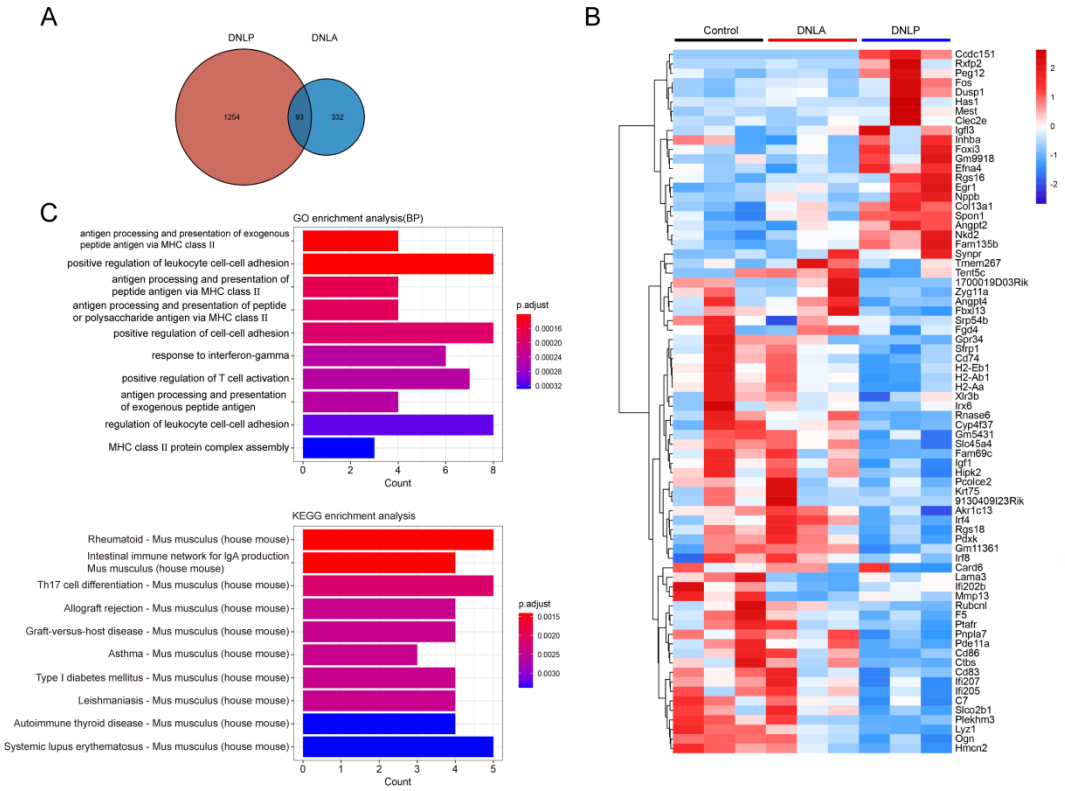

Figure 4: Comprehensive analysis of DEGs in psoriatic lesions of mice following DNLP/DNLA treatment. (A) Venn diagram of differentially expressed mRNAs from DNLP- and DNLA-treated groups. (B) Heatmap showing all differentially expressed mRNAs in skin lesions from DNLP- or DNLA-treated mice compared with control mice, for which all adjusted P-values < 0.05 and |Log2FC| > 1. (C) Top 10 enriched GO and KEGG pathways of DEGs.

3.5 DNLPs and DNLAs alleviated skin lesion inflammation through keratinocyte differentiation

Transcriptome sequencing analysis showed that DNLPs and DNLAs alleviated psoriasis lesions, primarily by modulating keratinocyte differentiation and myeloid leukocyte activation. K14 is expressed in the basal layer of normal skin and is associated with keratinocyte proliferation [36]. K16 and K17 are not expressed in the normal epidermis; however, when epidermal homeostasis is disrupted, their expression is strongly induced [37, 38]. The expression levels of K14, K16, and K17 are significantly elevated in psoriasis-like lesions and are correlated with disease severity [38]. Therefore, we examined the expression levels of K14 (Figure 5A, 5D), K16 (Figure 5B, 5E), and K17 (Figure 5C, 5F). Immunofluorescence results revealed that K14, K16, and K17 were downregulated following treatment with DNLPs and DNLAs, with DNLPs showing superior effects compared with DNLAs across all experiments.

ISSN 2706-6819 Vol.8, Issue 2: 11-24, DOI: 10.25236/IJFM.2026.080202

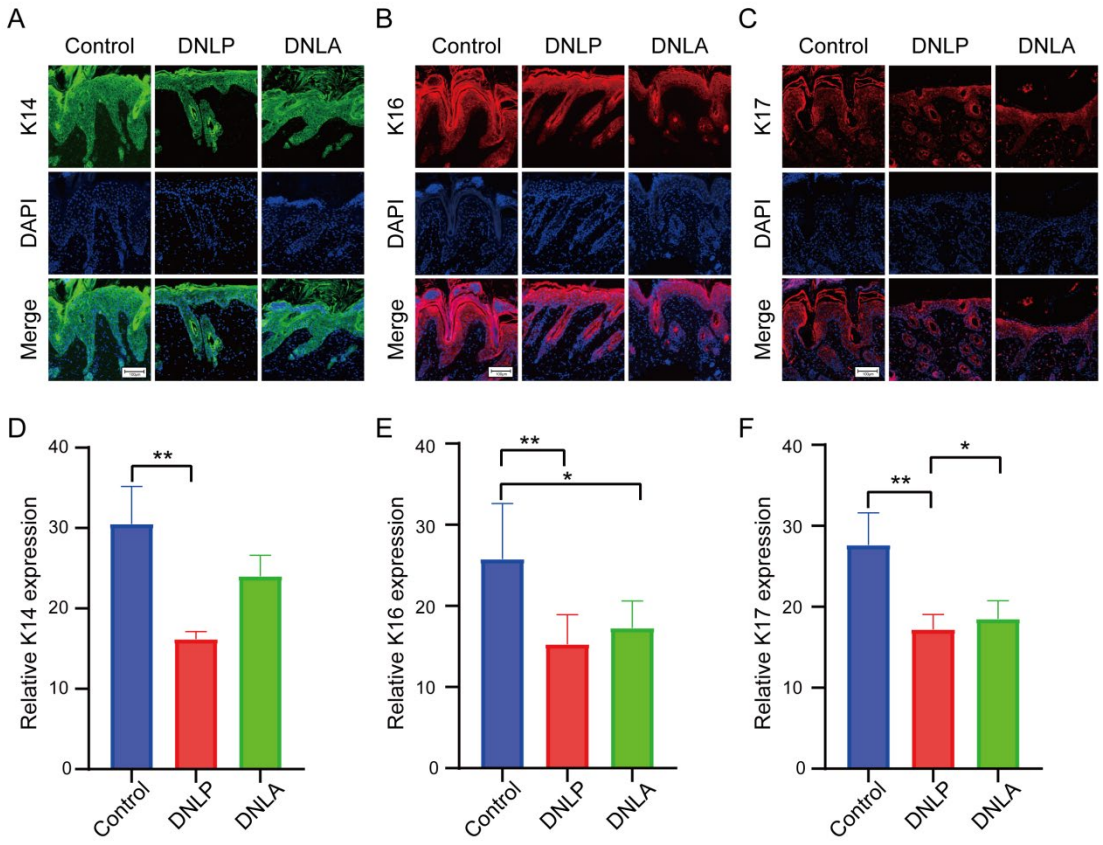

*Figure 5: DNLP/DNLA treatment inhibits the differentiation and proliferation of keratinocytes. (A–C) Immunostaining for keratin 14 (K14, A), keratin 16 (K16, B), and keratin 17 (K17, C) in psoriasiform skin lesions. Original magnification ×200, scale bar = 100 μm. (D–E) Quantitative analysis of the relative positive areas of K14, K16, and K17. Data are presented as mean ± SD. *P < 0.05, **P < 0.01; ns, not significant.*

3.6 DNLPs and DNLAs alleviated skin lesion inflammation through myeloid leukocyte activation

Next, we investigated myeloid cell infiltration using immunofluorescence staining. As shown in Figure 6, the M1 macrophage marker, iNOS (Figure 6A, 6C), exhibited a decreasing trend in the DNLP and DNLA groups, with a more significant reduction observed in the DNLA group. Similarly, the M2 macrophage marker, CD206 (Figure 6A, 6D), demonstrated a downward trend in the DNLP and DNLA groups, with a more pronounced decrease in the DNLA group. Additionally, we assessed the neutrophil marker Ly-6G (Figure 6B, 6E) and found a significant reduction in the number of Ly-6G-positive cells in the DNLP and DNLA groups. These findings are consistent with the RNA-seq results, suggesting that treatment with DNLPs and DNLAs alleviated psoriasis symptoms by reducing myeloid leukocyte infiltration.

ISSN 2706-6819 Vol.8, Issue 2: 11-24, DOI: 10.25236/IJFM.2026.080202

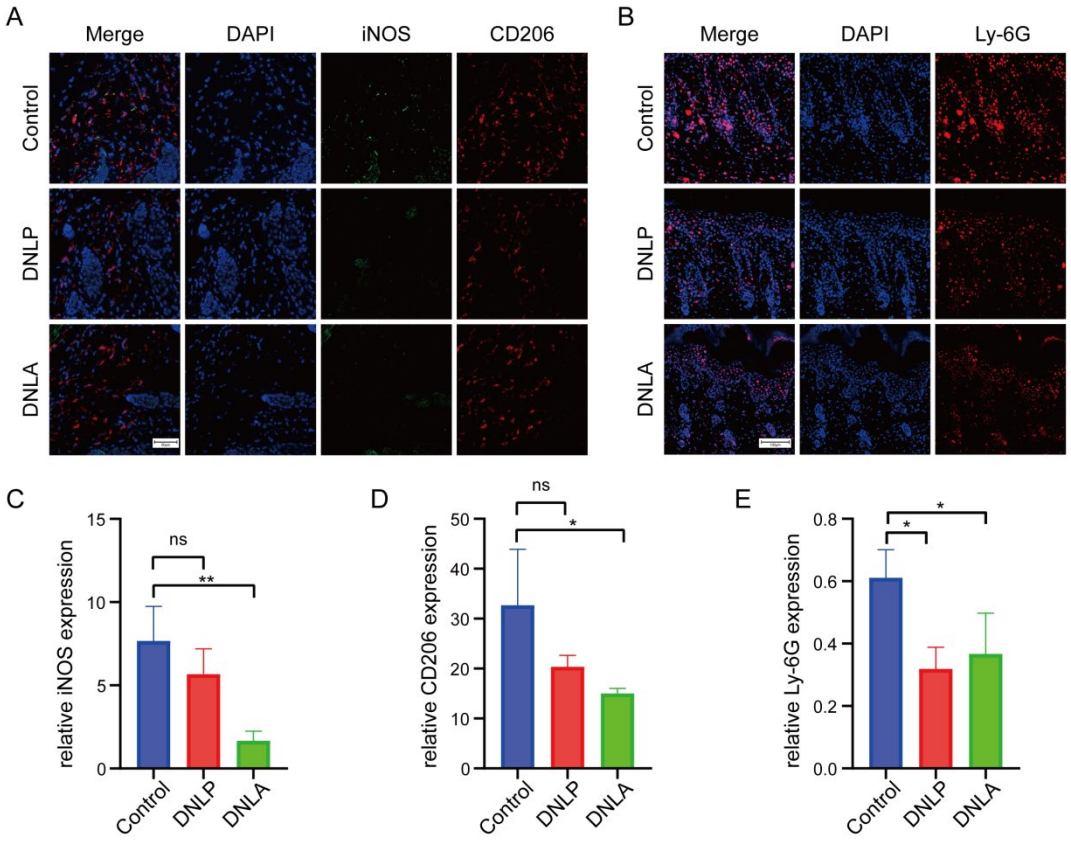

*Figure 6: DNLP/DNLA treatment inhibits myeloid cell infiltration. (A) Immunostaining for the M1 macrophage marker iNOS and the M2 macrophage marker CD206 in skin lesions. Original magnification ×400, scale bar = 50 μm. (B) Immunostaining for the neutrophil marker Ly-6G in skin lesions using tyramide signal amplification staining. Original magnification ×200, scale bar = 100 μm. (C, D) Quantitative analysis of iNOS- and CD206-positive cells. (E) Quantitative analysis of Ly-6G-positive cells. Data are presented as mean ± SD. *P < 0.05, **P < 0.01; ns, not significant.*

4. Discussion

Here, we demonstrated that DNLPs and DNLAs exhibited significant therapeutic effects in IMQ-induced psoriasis-like skin conditions. DNLPs and DNLAs effectively alleviated psoriasis symptoms by reducing epidermal thickness, erythema, and abnormal keratinocyte proliferation. Previous studies have reported that the expression levels of interleukins, such as IL-1, IL-6, IL-17a, IL-22, and IL-23, are significantly elevated in psoriatic lesional skin and IMQ-treated mouse skin [39]. Research has shown that the traditional herbal formula Dang-Gui-Liu-Huang Tang exerts anti-inflammatory effects by inhibiting the production of IL-22 in local skin lesions [40]. In our study, we found that DNLPs and DNLAs effectively reduced the expression of IL-17α and IL-1, as confirmed by IHC and qPCR. Additionally, RNA-seq analysis revealed a significant reduction in IL-6, IL-22, and IL-23 levels. Increasing evidence suggests that the IL-23/IL-17 axis plays a crucial role in the inflammatory cascade of psoriasis skin lesions, and blocking this axis can effectively reduce the interaction between Th17 cells and keratinocytes, making it a promising target for psoriasis therapy [15, 25]. Our study suggests that DNLPs and DNLAs downregulate cytokines, inhibit the abnormal proliferation of Th17 cells, and block the interaction between keratinocytes and Th17 cells, thereby improving psoriasis.

When we further investigated the potential targets of DNLPs and DNLAs for treating psoriasis, RNA-seq analysis provided deeper insights into the underlying molecular mechanisms by which DNLPs and DNLAs alleviate psoriasis-related skin inflammation. DNLPs significantly downregulate the expression of cytokines (e.g., IL-1β and IL-17α) and keratins, such as K5, K14, K16, and K17. The DEGs identified by RNA-seq were significantly enriched in immune-related pathways, including leukocyte migration, myeloid cell activation, and lysosomal and ribosomal functions, which play key roles in the immune regulation of inflammatory skin diseases [41-43]. Similarly, DNLAs significantly downregulated the expression of cytokines, K14, K16, K17, and S100 proteins. The DEGs were also enriched in immune-

ISSN 2706-6819 Vol.8, Issue 2: 11-24, DOI: 10.25236/IJFM.2026.080202

and inflammation-related pathways, including chemokine signalling and Th1, Th2, and Th17 cell differentiation. Notably, the analysis of common DEGs between the DNLP and DNLA treatment groups suggested that both drugs regulated the expression of genes related to antigen processing, intercellular adhesion, and T cell activation. These findings indicate that DNLPs and DNLAs share a common mechanism for regulating immune responses in psoriasis, likely through the modulation of keratinocyte differentiation and immune cell activation, thereby regulating the inflammatory processes of psoriasis.

Based on the results of transcriptome sequencing, we validated these findings using immunofluorescence. We found that, compared with those in the control group, samples from the DNLP and DNLA groups showed reduced expression of keratin markers (K14, K16, and K17) associated with the abnormal proliferation and differentiation of psoriatic keratinocytes [37, 38, 44]. The expression levels of the M1 macrophage marker iNOS, M2 macrophage marker CD206, and neutrophil marker Ly-6G decreased compared with those in the control group, indicating that DNLPs and DNLAs affect myeloid cell infiltration. Therefore, we hypothesise that DNLPs and DNLAs have dual effects on keratinocytes and immune cells, thereby influencing inflammatory processes in psoriasis.

Our results showed a significant reduction in iNOS (M1 macrophages), CD206 (M2 macrophages), and Ly-6G (neutrophils) levels, indicating suppression of myeloid leukocyte infiltration. Notably, M1 macrophages are typically associated with pro-inflammatory responses, whereas M2 macrophages are involved in tissue repair and have anti-inflammatory effects [45, 46]. The synchronous reduction in both cell populations suggests a shift in macrophage polarisation, which may not represent a simple transition from a pro-inflammatory to an anti-inflammatory state. Rather than merely suppressing infiltration, this phenomenon could be interpreted as the reprogramming of myeloid cells, thereby achieving a more balanced immune microenvironment. Furthermore, given the inflammatory drive for myeloid cell recruitment and activation, these alterations may reflect the secondary effects of resolving inflammation.

Current research suggests that many TCHs regulate the key signalling pathways involved in psoriasis. An in vitro study by Xu et al. showed that Jingfang granules target keratinocytes by binding to PPARγ, p38a MAPK, and TNF-α, inhibiting bone marrow-derived dendritic cell maturation, and reducing NF-κB/STAT3 activity in keratinocytes via the p38a MAPK signalling pathway [14]. In another study, imperatorin isolated from *Angelica hirsutiflora* inhibited PDE4 activity in human neutrophils and increased cAMP levels. This increase in cAMP levels exerts anti-inflammatory effects by inhibiting Akt, extracellular signal-regulated kinase (ERK), c-Jun NH2-terminal kinase (JNK), and Ca^{2+} [12].

In this study, we investigated the potential signalling pathways through which DNLPs and DNLAs exert their effects. Despite adaptive immune dysregulation, psoriasis inflammation typically presents with a localised distribution pattern. The S100A8/S100A9 heterodimers are damage-associated molecular patterns (DAMPs) that play a critical role in local inflammation and activate immune responses by binding to the TLR4/MD2 complex in the immune system, thereby triggering local inflammatory responses [47]. Blocking the TLR4-binding site of active S100 dimers represents a promising approach for the local suppression of inflammatory diseases while avoiding systemic side effects. DNLPs play an immunomodulatory role by binding to the TLR4-MD2 complex and blocking the MAPK/NF-κB signalling pathway, thus regulating immune cell function [48]. The MAPK family includes p38 MAPK, ERK, and JNK, all of which play important roles in psoriasis [49]. Many signals (e.g., DAMPs, CCN1, and IL-22) in psoriasis can activate the JNK pathway in keratinocytes. The activated JNK pathway in keratinocytes mediates the recruitment of immune cells in psoriasis by regulating the production of inflammatory chemokines, such as IL-6, IL-8, IL-23, interferon-γ, and TNF-α [39, 50]. The NF-κB pathway also plays a crucial role in psoriasis, as it alters the behaviour of keratinocytes and immune cells by affecting their proliferation, differentiation, and the production of cytokines or chemokines [51, 52]. In our study, DNLPs and DNLAs significantly reduced keratinocyte proliferation, expression of inflammatory cytokines, and immune cell differentiation, activation, and adhesion in a mouse model of psoriasis. Based on the findings of this study and reports in the existing literature, we hypothesise that DNLPs and DNLAs exert their therapeutic effects by binding to the TLR4/MD2 complex and inhibiting the MAPK/NF-κB signalling pathway. However, direct experimental validation is required to confirm this mechanism, such as by assessing the expression levels of TLR4/MD2 and the phosphorylation/activation status of key signalling proteins, including p38, JNK, ERK, and NF-κB p65. Future studies should consider employing pharmacological inhibition or genetic approaches to further explore this hypothesis.

Overall, the observed downregulation of pro-inflammatory cytokines and chemokines, along with the modulation of pathways involved in immune cell infiltration, suggests that DNLPs and DNLAs alleviate psoriatic inflammation by regulating the activity and infiltration of myeloid leukocytes. This is consistent with previous findings indicating that myeloid leukocytes, including macrophages and dendritic cells, play a pivotal role in the pathogenesis of psoriasis by producing cytokines that activate T cells and

ISSN 2706-6819 Vol.8, Issue 2: 11-24, DOI: 10.25236/IJFM.2026.080202

promote inflammation [53, 54]. DNLPs and DNLAs reduce the activation and recruitment of these immune cells, thereby restoring balance in the psoriatic microenvironment and mitigating inflammation.

In summary, our results indicate that DNLPs and DNLAs significantly alleviate IMQ-induced psoriasiform skin inflammation by inhibiting the abnormal proliferation and differentiation of keratinocytes and modulating myeloid cell activation. Therefore, this study provides valuable insights into psoriasis treatment and suggests that future research could lead to the development of new therapeutic strategies. Nevertheless, this study has certain limitations. Although the keratin markers K14, K16, and K17 effectively reveal phenotypic alterations associated with keratinocyte differentiation, they do not fully elucidate the mechanistic basis of the action of DNLPs/DNLAs. To address this issue, we reviewed relevant literature on the transcriptional regulatory mechanisms of keratinocyte differentiation. Key transcription factors (such as p63) and components of the Notch signalling pathway are crucial for keratinocyte differentiation and their response to environmental signals [55-58]. Although this study did not specifically analyse these factors, we hypothesise that the observed downregulation of keratin markers may result from alterations in these regulatory pathways. Subsequent experiments should focus on validating this hypothesis, thereby incorporating key transcriptional regulators such as p63 and Notch signalling into the marker system for keratinocyte differentiation.

Although previous studies have reported that psoriasis results from crosstalk between keratinocytes and immune cells, leading to amplified inflammatory cascades [59, 60], our study confirmed that DNLPs and DNLAs affect both cell types. However, our study did not investigate the precise interrelationship between keratinocytes and immune cells, whether they act concurrently, or if they dominate the regulation of the inflammatory process in psoriasis. However, further investigation is required in this regard. Furthermore, when designing our experiments, we referred to studies on other *Dendrobium* species, which indicated that *Dendrobium officinale* polysaccharides do not affect the proliferation of normal keratinocytes [61]. However, we did not establish a control group of normal skin treated with DNLPs/DNLAs to investigate the effects of these compounds on epidermal proliferation, differentiation, and immune cell distribution in a non-inflammatory state. This represents a lack of rigour.

5. Conclusion

Consistent with previous preliminary reports, our data strongly indicate that Dendrobium extract (containing alkaloids and polysaccharides) exerts significant anti-inflammatory effects. In the IMQ-induced psoriasis model, systemic administration of DNLPs and DNLAs effectively inhibited abnormal keratinocyte proliferation and differentiation and reduced inflammatory cell infiltration, myeloid leukocyte activation, and other indicators, thereby restoring the balance of the inflammatory microenvironment and improving the disease phenotype and PASI scores.

Acknowledgement

This work was supported by the National Natural Science Foundation of China (32160175), the PhD Fund of Scientific Research Foundation of School and Hospital of Stomatology, Zunyi Medical University (no. KY2020-14).

References

[1] Armstrong A W, Read C. Pathophysiology, Clinical Presentation, and Treatment of Psoriasis A Review [J]. JAMA-J Am Med Assoc, 2020, 323(19): 1945-1960.
[2] Michalek I M, Loring B, John S M. A systematic review of worldwide epidemiology of psoriasis [J]. J Eur Acad Dermatol Venereol, 2017, 31(2): 205-212.
[3] Michalek I, Loring B, John S. WHO Global report on psoriasis [M]. Geneva, Switzerland: World Health Organization. 2016.
[4] Griffiths C E M, Armstrong A W, Gudjonsson J E, Barker J. Psoriasis [J]. Lancet, 2021, 397(10281): 1301-1315.
[5] Boehncke W H, Schön M P. Psoriasis [J]. Lancet, 2015, 386(9997): 983-994.
[6] Lee H J, Kim M. Challenges and Future Trends in the Treatment of Psoriasis [J]. Int J Mol Sci, 2023, 24(17).
[7] Li T, Gao S, Han W, et al. Potential effects and mechanisms of Chinese herbal medicine in the treatment of psoriasis [J]. J Ethnopharmacol, 2022, 294: 115275.

ISSN 2706-6819 Vol.8, Issue 2: 11-24, DOI: 10.25236/IJFM.2026.080202

[8] Meng S, Lin Z, Wang Y, et al. Psoriasis therapy by Chinese medicine and modern agents [J]. Chin Med, 2018, 13: 16.
[9] Lai R, Xian D, Xiong X, et al. Proanthocyanidins: novel treatment for psoriasis that reduces oxidative stress and modulates Th17 and Treg cells [J]. Redox Rep, 2018, 23(1): 130-135.
[10] Kim B S, Lu H, Ichiyama K, et al. Generation of RORγt(+) Antigen-Specific T Regulatory 17 Cells from Foxp3(+) Precursors in Autoimmunity [J]. Cell Rep, 2017, 21(1): 195-207.
[11] Wu A, Wang Y, Mao R, et al. Naturally-occurring carnosic acid as a promising therapeutic agent for skin inflammation via targeting STAT1 [J]. Phytomedicine, 2025, 139: 156442.
[12] Xu Q, Sheng L, Zhu X, et al. Jingfang granules exert anti-psoriasis effect by targeting MAPK-mediated dendritic cell maturation and PPARγ-mediated keratinocytes cell cycle progression in vitro and in vivo [J]. Phytomedicine, 2023, 117: 154925.
[13] Sarkar D, Gorai P, Pramanik A, et al. Characterization and active component identification of Premna herbacea roxb. root extract reveals anti-inflammatory effect and amelioration of imiquimod induced psoriasis via modulation of macrophage inflammatory response [J]. Phytomedicine, 2023, 119: 155007.
[14] Tsai Y F, Chen C Y, Lin I W, et al. Imperatorin Alleviates Psoriasiform Dermatitis by Blocking Neutrophil Respiratory Burst, Adhesion, and Chemotaxis Through Selective Phosphodiesterase 4 Inhibition [J]. Antioxid Redox Signal, 2021, 35(11): 885-903.
[15] Jeon Y J, Sah S K, Yang H S, et al. Rhododendrin inhibits toll-like receptor-7-mediated psoriasis-like skin inflammation in mice [J]. Exp Mol Med, 2017, 49(6): e349.
[16] Chao W H, Lai M Y, Pan H T, et al. Dendrobium nobile Lindley and its bibenzyl component moscatilin are able to protect retinal cells from ischemia/hypoxia by dowregulating placental growth factor and upregulating Norrie disease protein [J]. BMC Complement Altern Med, 2018, 18(1): 193.
[17] Huang J, Huang N, Zhang M, et al. Dendrobium alkaloids decrease Aβ by regulating α- and β-secretases in hippocampal neurons of SD rats [J]. PeerJ, 2019, 7: e7627.
[18] Mou Z, Zhao Y, Ye F, et al. Identification, Biological Activities and Biosynthetic Pathway of Dendrobium Alkaloids [J]. Front Pharmacol, 2021, 12: 605994.
[19] Fan C, Sun X, Wang X, Yu H. Therapeutic potential of the chemical composition of Dendrobium nobile Lindl [J]. Front Pharmacol, 2023, 14: 1163830.
[20] Morita A. Current developments in phototherapy for psoriasis [J]. J Dermatol, 2018, 45(3): 287-292.
[21] Wang R, Bi Y, Xie Y, et al. Dendrobium nobile Lindl. Polysaccharides ameliorate the inflammatory microenvironment in the retina of diabetic rats: a multi-omics study of the gut-blood-retina axis [J]. Int J Biol Macromol, 2025, 316(Pt 1): 144732.
[22] Zhang S, Tu H, Zhu J, et al. Dendrobium nobile Lindl. polysaccharides improve follicular development in PCOS rats [J]. Int J Biol Macromol, 2020, 149: 826-834.
[23] Xu Y Y, Xu Y S, Wang Y, et al. Dendrobium nobile Lindl. alkaloids regulate metabolism gene expression in livers of mice [J]. J Pharm Pharmacol, 2017, 69(10): 1409-1417.
[24] Nie J, Jiang L S, Zhang Y, et al. Dendrobium nobile Lindl. Alkaloids Decreases the Level of Intracellular β-Amyloid by Improving Impaired Autolysosomal Proteolysis in APP/PS1 Mice [J]. Front Pharmacol, 2018, 9: 1479.
[25] Van Der Fits L, Mourits S, Voerman J S, et al. Imiquimod-induced psoriasis-like skin inflammation in mice is mediated via the IL-23/IL-17 axis [J]. J Immunol, 2009, 182(9): 5836-5845.
[26] Gangwar R S, Gudjonsson J E, Ward N L. Mouse Models of Psoriasis: A Comprehensive Review [J]. J Invest Dermatol, 2022, 142(3 Pt B): 884-897.
[27] Miller I, Min M, Yang C, et al. Ki67 is a Graded Rather than a Binary Marker of Proliferation versus Quiescence [J]. Cell Rep, 2018, 24(5): 1105-1112.e5.
[28] Rendon A, Schäkel K. Psoriasis Pathogenesis and Treatment [J]. Int J Mol Sci, 2019, 20(6).
[29] Rutkowski E, Leibelt S, Born C, et al. Clr-a: A Novel Immune-Related C-Type Lectin-like Molecule Exclusively Expressed by Mouse Gut Epithelium [J]. J Immunol, 2017, 198(2): 916-926.
[30] Li Z, Ju X, Silveira P A, et al. CD83: Activation Marker for Antigen Presenting Cells and Its Therapeutic Potential [J]. Front Immunol, 2019, 10: 1312.
[31] Zhao Y, Xiong J, Chen H X, et al. A Spontaneous H2-Aa Point Mutation Impairs MHC II Synthesis and CD4(+) T-Cell Development in Mice [J]. Front Immunol, 2022, 13: 810824.
[32] Zhang Y H, Sun X T, Guo R F, et al. AβPP-tau-HAS1 axis trigger HAS1-related nuclear speckles and gene transcription in Alzheimer's disease [J]. Matrix Biol, 2024, 129: 29-43.
[33] Wang H N, Ji K, Zhang L N, et al. Inhibition of c-Fos expression attenuates IgE-mediated mast cell activation and allergic inflammation by counteracting an inhibitory AP1/Egr1/IL-4 axis [J]. J Transl Med, 2021, 19(1): 261.
[34] Yang J, Sun L, Han J, et al. DUSP1/MKP-1 regulates proliferation and apoptosis in keratinocytes

ISSN 2706-6819 Vol.8, Issue 2: 11-24, DOI: 10.25236/IJFM.2026.080202

through the ERK/Elk-1/Egr-1 signaling pathway [J]. Life Sci, 2019, 223: 47-53.
[35] Diani M, Perego S, Sansoni V, et al. Differences in Osteoimmunological Biomarkers Predictive of Psoriatic Arthritis among a Large Italian Cohort of Psoriatic Patients [J]. Int J Mol Sci, 2019, 20(22).
[36] Hovnanian A, Pollack E, Hilal L, et al. A missense mutation in the rod domain of keratin 14 associated with recessive epidermolysis bullosa simplex [J]. Nat Genet, 1993, 3(4): 327-332.
[37] Lin Y, Zhang W, Li B, Wang G. Keratin 17 in psoriasis: Current understanding and future perspectives [J]. Semin Cell Dev Biol, 2022, 128: 112-119.
[38] Zhang X, Yin M, Zhang L J. Keratin 6, 16 and 17-Critical Barrier Alarmin Molecules in Skin Wounds and Psoriasis [J]. Cells, 2019, 8(8).
[39] Guo J, Zhang H, Lin W, et al. Signaling pathways and targeted therapies for psoriasis [J]. Signal Transduct Target Ther, 2023, 8(1): 437.
[40] Nguyen L T H, Ahn S H, Nguyen U T, Yang I J. Dang-Gui-Liu-Huang Tang a traditional herbal formula, ameliorates imiquimod-induced psoriasis-like skin inflammation in mice by inhibiting IL-22 production [J]. Phytomedicine, 2018, 47: 48-57.
[41] Reynolds G, Vegh P, Fletcher J, et al. Developmental cell programs are co-opted in inflammatory skin disease [J]. Science, 2021, 371(6527).
[42] Mehta H, Angsana J, Bissonnette R, et al. Inflammatory Skin Disorders: Monocyte-Derived Cells Take Center Stage [J]. Front Immunol, 2021, 12: 691806.
[43] Chen L, Shen Z. Tissue-resident memory T cells and their biological characteristics in the recurrence of inflammatory skin disorders [J]. Cell Mol Immunol, 2020, 17(1): 64-75.
[44] Luo Y, Pang B, Hao J, et al. Keratin 17 covalently binds to alpha-enolase and exacerbates proliferation of keratinocytes in psoriasis [J]. Int J Biol Sci, 2023, 19(11): 3395-3411.
[45] Murray P J, Wynn T A. Protective and pathogenic functions of macrophage subsets [J]. Nat Rev Immunol, 2011, 11(11): 723-737.
[46] Mosser D M, Edwards J P. Exploring the full spectrum of macrophage activation [J]. Nat Rev Immunol, 2008, 8(12): 958-969.
[47] Vogl T, Stratis A, Wixler V, et al. Autoinhibitory regulation of S100A8/S100A9 alarmin activity locally restricts sterile inflammation [J]. J Clin Invest, 2018, 128(5): 1852-1866.
[48] Li L, Chen H, Huang G, et al. Structure of Polysaccharide from Dendrobium nobile Lindl. and Its Mode of Action on TLR4 to Exert Immunomodulatory Effects [J]. Foods, 2024, 13(9).
[49] Kim E K, Choi E J. Pathological roles of MAPK signaling pathways in human diseases [J]. Biochim Biophys Acta, 2010, 1802(4): 396-405.
[50] Hammouda M B, Ford A E, Liu Y, Zhang J Y. The JNK Signaling Pathway in Inflammatory Skin Disorders and Cancer [J]. Cells, 2020, 9(4).
[51] Zhou X, Chen Y, Cui L, et al. Advances in the pathogenesis of psoriasis: from keratinocyte perspective [J]. Cell Death Dis, 2022, 13(1): 81.
[52] Andres-Ejarque R, Ale H B, Grys K, et al. Enhanced NF-κB signaling in type-2 dendritic cells at baseline predicts non-response to adalimumab in psoriasis [J]. Nat Commun, 2021, 12(1): 4741.
[53] Sieminska I, Pieniawska M, Grzywa T M. The Immunology of Psoriasis-Current Concepts in Pathogenesis [J]. Clin Rev Allergy Immunol, 2024, 66(2): 164-191.
[54] Prinz J C. The role of T cells in psoriasis [J]. J Eur Acad Dermatol Venereol, 2003, 17(3): 257-270.
[55] Nguyen B C, Lefort K, Mandinova A, et al. Cross-regulation between Notch and p63 in keratinocyte commitment to differentiation [J]. Genes Dev, 2006, 20(8): 1028-1042.
[56] Tadeu A M, Horsley V. Notch signaling represses p63 expression in the developing surface ectoderm [J]. Development, 2013, 140(18): 3777-3786.
[57] Kouwenhoven E N, Oti M, Niehues H, et al. Transcription factor p63 bookmarks and regulates dynamic enhancers during epidermal differentiation [J]. EMBO Rep, 2015, 16(7): 863-878.
[58] Siebel C, Lendahl U. Notch Signaling in Development, Tissue Homeostasis, and Disease [J]. Physiol Rev, 2017, 97(4): 1235-1294.
[59] Kamata M, Tada Y. Crosstalk: keratinocytes and immune cells in psoriasis [J]. Front Immunol, 2023, 14: 1286344.
[60] Albanesi C, Madonna S, Gisondi P, Girolomoni G. The Interplay Between Keratinocytes and Immune Cells in the Pathogenesis of Psoriasis [J]. Front Immunol, 2018, 9: 1549.
[61] Zeng B, Yan Y, Zhang Y, et al. Dendrobium officinale Polysaccharide (DOP) inhibits cell hyperproliferation, inflammation and oxidative stress to improve keratinocyte psoriasis-like state [J]. Adv Med Sci, 2024, 69(1): 167-175.